



**university of
 groningen**

**faculty of science
 and engineering**

Integration Project Report:

Silicon nitride PVD coating as electron blocking layer for high-performance triboelectric nanogenerator

1st supervisor: Prof. dr. Y. (Yutao) Pei

2nd supervisor: dr. A.J. (Albert) Bosch

And

daily supervisor: W. (Wenjian) Li

Niels Glasbergen (S4039114)

July 1, 2023

Abstract

Triboelectric nanogenerators (TENG) are small energy-harvesting devices that convert mechanical energy into electrical energy by creating triboelectrification. TENGs have the potential for broad applications in medical science, human interactions and energy sources. The broad range of material selection provides the potential to generate high quantities of electricity and to be applicable in different environments. However, occurring regional electrical breakdowns are affecting the TENG's performance. To solve this problem, this project investigated the use of an intermediate layer. The intermediate layer will function as an electron-blocking layer (EBL) that will prevent electrical breakdowns. This project concentrates on Silicon Nitrate (Si_3N_4) as an EBL to enhance the output of the TENG. The Si_3N_4 coating needs to balance between blocking and transporting the electrons for the TENG to enhance its performance, which is done by finding the optimal thickness for the Si_3N_4 layer. The performances of the intermediate layer are assessed in open circuit voltage (Voc), short circuit current (Isc) and short circuit transferred charge (Qsc). This research showed an increased performance of 20-30% in all variables with a thickness roughly around 346.5 nm compared to the previously researched performances with a Si_3N_4 as EBL.

Contents

	Page
List of Abbreviations	5
1 Introduction	6
2 TENG mechanism	7
3 Literature review	8
3.1 Triboelectricity	8
3.2 Output of the TENG	10
3.2.1 Accumulation and decay time	11
3.3 Electrical breakdowns	12
4 Problem analysis	13
4.1 Problem context	13
4.2 Holistic system	13
4.3 Research objective	14
4.4 Research questions	14
5 Intermediate layer	15
5.1 Design	15
5.2 The effects of an intermediate layer	16
5.3 Characteristics of materials	17
5.3.1 Silicon nitride	17
5.3.2 Polydimethylsiloxane	17
5.3.3 Copper and titanium	17
6 Equipment	18
6.1 Physical Vapour Deposition	18
6.2 Spin-coating	18
6.3 Electrometer	18
6.4 Tensile tester	18
7 Results and discussion	19
7.1 Coatings	19
7.1.1 Electrodes and Si_3N_4	19
7.1.2 PDMS	22
7.2 Output results	23
7.2.1 Results with $11\mu\text{m}$ PDMS coating	23
7.2.2 Results with $15\sim 20\mu\text{m}$ PDMS coating	25
7.3 Discussion	28
8 Applications of TENG	32
9 Conclusion	33

Bibliography	34
Appendices	37
A Equipment used	37
B Results Bas Veenstra	38
Acknowledgement	39

List of Abbreviations

TENG - Triboelectric Nanogenerator

CS-TENG - Contact-Separation Triboelectric Nanogenerator

IoT - Internet of Things

ENTEGR - Engineering and Technology Institute Groningen

APE - Advanced Production Engineering

SiN - Silicon Nitride

Cu - Copper

Ti - Titanium

PDMS - Polydimethylsiloxane

PVD - physical vapour deposition

Voc - Open-Circuit Voltage

Isc - Short-Circuit Current

Qsc - Short-Circuit Charge

1 Introduction

Energy is indispensable for modern civilisation, however, 60% of all energy in Europe is still generated using fossil fuels [Martins et al., 2019]. Fossil fuels lead to climate change, air pollution, and environmental degradation, posing significant hazards to our planet and future generations. This can be prevented by using renewable and clean energy sources. Converting mechanical energy into electricity is currently done using, among others, windmills or hydroelectric power on a large scale. A new way to convert mechanical energy on a small scale is via a triboelectric nanogenerator (TENG). Wang et al. created the TENG roughly ten years ago and it has since been actively investigated due to its versatility and great potential. The TENG creates the triboelectric effect, which is a type of contact electrification, by creating a potential difference between the two materials. This potential difference results in electrons moving from one material to the other, which can be harvested into electricity. The TENG is a promising innovation due to its low cost, high reliability and diverse choice of materials [Wu et al., 2019]. Moreover, it has the potential to be broadly applicable for both large-scale energy harvesting and as an energy source for tiny electronic devices [Martins et al., 2019]. The application of renewable energy sources for tiny electronic devices has an increasing demand due to, among others, the Internet of Things (IoT). The advantage of the IoT is that objects can make their own decisions without human interaction. Right now, the Internet of Things is present in almost every sector and will be an indispensable innovation that will be implemented on an even broader scale [Rudra et al., 2022]. The IoT uses sensors to monitor and measure various physical phenomena and transfer them to cloud-based systems for analysis. The current standard for the energy source of the sensors is non-renewable batteries, which are the cause of environmental degradation, as well as raising concerns about human rights violations in the extraction of critical minerals such as lithium [Akhtar and Rehmani, 2015]. Moreover, the batteries can be inconvenient as they need to be charged or replaced at a certain point. This can be solved by using TENGs instead of batteries. However, TENGs are currently not providing enough output voltage for the sensors and are commonly used in combination with another renewable energy source. This integration project investigates how the inclusion of an intermediate layer will influence and possibly enhance the performance of the TENG.

2 TENG mechanism

There are four distinct TENG modes: sliding, free-standing, one electrode and the contact separation mode. The contact-separation TENG (CS-TENG) is used in this project because it is the least complex mode and can consist of either three or four layers. For the four-layer design, two dielectric materials are deposited on the electrodes and face each other. In the three-layer design, there is only one electrode coated with a dielectric material. In the initial state of the system, both components are separated. An applied external mechanical force will press the top electrode against the bottom component. The connection between the different materials causes contact electrification. Resulting in a potential difference when separated again. The difference generates triboelectricity between the electrodes, causing electricity to go through the wire. All of the modes have three distinct stages: contacting, contacted and separating [Xie et al., 2021]. The various phases are projected in the contact-separation mode in Figure 1.

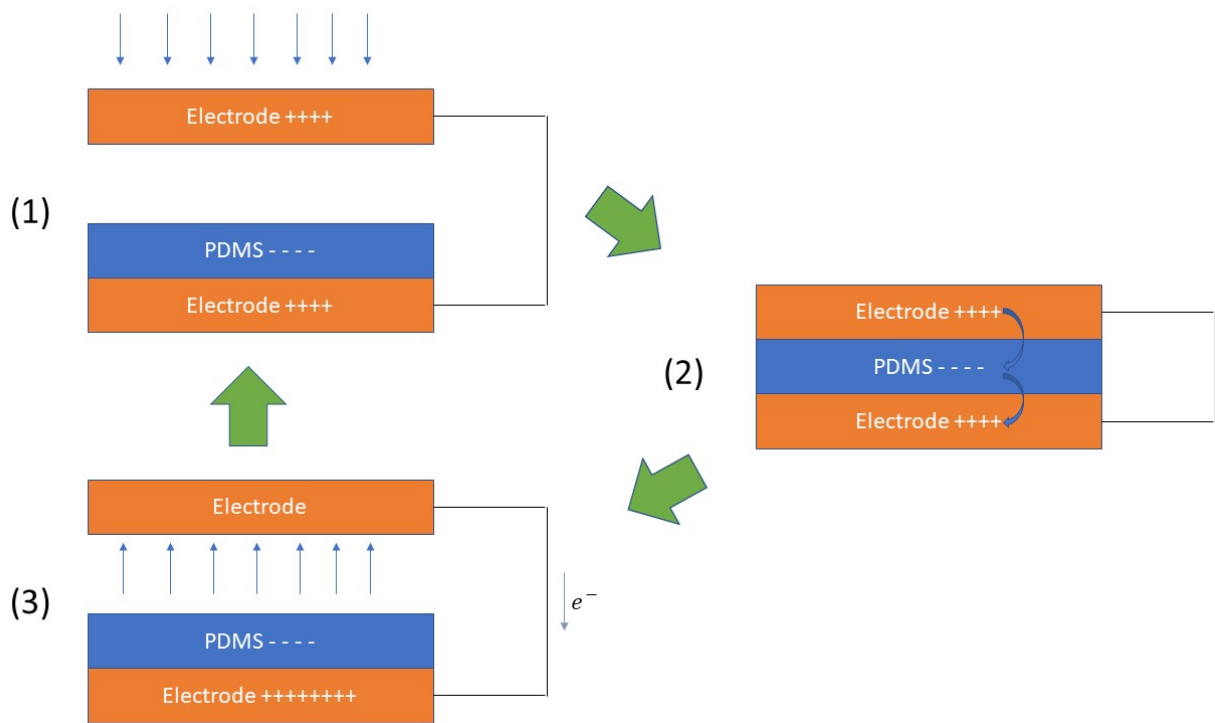


Figure 1: Triboelectric nanogenerator system stages: (1) contacting, (2) contacted, (3) separating

3 Literature review

3.1 Triboelectricity

The development of the TENG is based on Maxwell's displacement current, which begins with Ampere's circuital law and Maxwell's addition in the following formula:

$$\nabla * H = J_f + \frac{\partial D}{\partial t} \quad (1)$$

where H is the magnetizing field, J_f is the free electric current density and D is the displacement field. Where D can be defined as

$$D = \epsilon_0 E + P \quad (2)$$

where E is the electric field, P is the polarization field and ϵ_0 is the vacuum permittivity. Now the second term in equation 1 can be defined as:

$$J_D = \frac{\partial D}{\partial t} = \epsilon_0 \frac{\partial E}{\partial t} + \frac{\partial P}{\partial t} \quad (3)$$

this equation is known as the displacement current which consists of two terms. The first term $\epsilon_0 \frac{\partial E}{\partial t}$ associates the magnetic field with actual current, which is used to develop radio, TV and other long-distance communication devices [Wang, 2017]. The second term $\frac{\partial P}{\partial t}$ is the base for the output signal of nanogenerators, which is fundamental for the use of TENG- driven sensors.

The triboelectric nanogenerators that are based on the contact separation have the following formula corresponding to the current displacement according to Wang et al.:

$$J_D = \sigma_c \frac{dz}{dt} \frac{d_1 * \epsilon_0 / \epsilon_1 + d_2 * \epsilon_0 / \epsilon_2}{[d_1 * \epsilon_0 / \epsilon_1 + d_2 * \epsilon_0 / \epsilon_2 + z]^2} \quad (4)$$

where d is the thickness of the dielectric, z is the gap distance between contact separation and σ_c the accumulation of the free electrodes. The accumulation will be explained further in section 3.2.1. Permittivity is a factor that is receptively used in the fundamentals of the TENG. The permittivity of the dielectric material used in a TENG influences its ability to polarize when exposed to an electric field. Increased permittivity allows the dielectric to store more charge, resulting in improved polarisation and increased voltage output in the TENG. This means that for the material selection, permittivity is a major factor determining the dielectric of the TENG.

Triboelectrification can be generated through solid-liquid, solid-gas, liquid-gas and solid-solid contact between materials. Articles on triboelectrification are mostly based on experimental outcomes rather than the actual underlying physics. Even though the TENG is based on Maxwell's displacement current, its research about which charge species transfer during triboelectrification has yet to be theorized [Kim et al., 2021]. However, three categories of possible charge species transfer mechanisms can cause triboelectricity: electron transfers, ion transfers, and cleaved bulk transfers. For electron transfers, it is the contact pairs that cause the charge difference. This type firmly hinges on the work function difference between the materials. Meaning that there is a difference in the quantity of electricity that it takes to remove an electron from the uncharged surface. For ion transfers, contact between materials can cause ions to transfer from one material to the other; this separation causes triboelectricity. The cleaved bulk transfers are considered not to be the primary mechanism underpinning triboelectricity, but it has been discovered that some material transfers occur [Kim et al., 2021]. This project is based on the electron transfer mechanism since the work functions can be found instead of using complex measuring machines to find ion and material transfers.

3.2 Output of the TENG

There are two distinct varieties of TENGs regarding current: direct current (DC) and alternating current (AC) TENGs. Most TENGs create AC, such as the CS-TENG, which needs to be converted into DC to make the TENG suitable for storing and driving electrical devices [Song et al., 2020]. This is usually done by using a rectifier, which can convert AC to DC. Using a rectifier decreases the output of the TENG, hence a depletion in its performance.

The output current between the two surfaces of the TENG can be estimated using the following equation:

$$I = \frac{dQ}{dt} \quad (5)$$

where I is the output current, and $\frac{dQ}{dt}$ is the rate of change of charge with respect to time. The output charge of a TENG can be calculated using the following formula:

$$Q = C * V \quad (6)$$

where Q is the charge generated, C is the capacitance of the TENG, and V is the voltage generated. Where the capacitance of a TENG is the maximum amount of electricity it can store.

There are three distinct variables measured to indicate the performance of a CS-TENG. The open circuit voltage (V_{oc}) is the maximal voltage measured between the two electrodes in V, which in the TENG is at its upper limit when entirely separated. The short circuit current (I_{sc}) is the maximal current in mA, which is measured immediately after the separation because it yields its maximum potential difference at that point. Thirdly, there is the short-circuit transferred charge (Q_{sc}) which is the amount of transferred charge in nC and is highest when the TENG is in contact. All of these variables are depicted in Figure 2 and can be measured using an electrometer in combination with Wenjian's Python script.

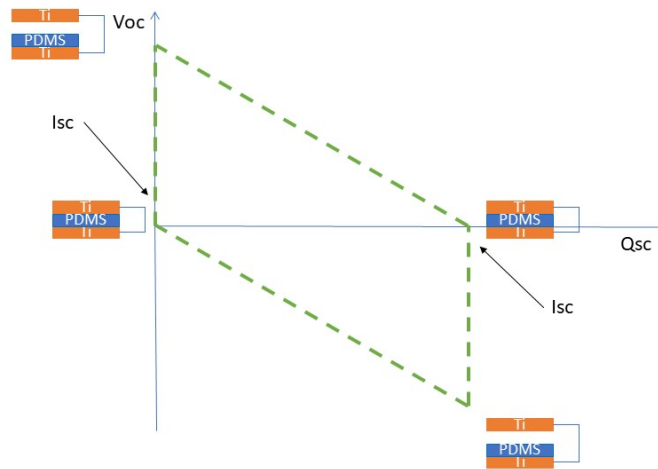


Figure 2: Schematic overview of the output in a CS-TENG

3.2.1 Accumulation and decay time

When the TENG begins the contact separation movement, it does not instantaneously generate the highest output. This is because the triboelectric charges on the surfaces of the triboelectric layers need to increase. After each cycle of contact separation, the TENG increases its potential difference until it reaches an equilibrium. What happens is that the charge cavities in the electrode layer need to be filled in with electrons, which is called accumulation. Higher accumulation means that the cavities are filled faster with electrons, resulting in a faster optimal potential difference. This can be optimal for a TENG that is in an environment where the TENG is on hold for a long time and needs to generate power in a short time.

Next to the accumulation time is the decay time, the time it takes for a TENG to go back to the original potential difference when it ceases the contact separation cycles. This period is desired to be very long so the TENG can reach its maximum output faster when resuming the motion. Both accumulation and decay have been tested by Cui et al. with and without an intermediate layer, where the accumulation took around the same time, even when the output increased substantially. Moreover, the decay time was tested in the experiment, which went from 22 min to 44 hours when introducing an intermediate layer. This demonstrates a remarkable improvement in performance when adding an intermediate layer.

3.3 Electrical breakdowns

The regional electrical breakdowns decreases the performance of the TENG. The TENG is experiencing regional electrical breakdowns due to the low breakdown voltage of the dielectric, which is caused by the thickness of the dielectric. An electrical breakdown happens when a voltage higher than the breakdown voltage is applied across an insulating material. The material ionizes and a current can travel through the material, manifesting as an electrostatic discharge [Deshmukh et al., 2020] [Ruys, 2018]. When the dielectric material is very thin, the electrical breakdown voltage decreases linearly with its thickness [Neusel et al., 2015]. Resulting in the following formula that can be used to determine the electrical breakdown voltage of a material.

$$V_b = t * E_{ds} \quad (7)$$

In this equation, V_b is the electrical breakdown voltage, t is the thickness of the material and E_{ds} is the dielectric strength. The dielectric strength is defined as the electrical strength of a dielectric material, signifying the limit at which the material is still acting as an insulator. There are several factors that affect the performance of the TENG. First, the low thickness of the dielectric layer is causing the electrical breakdown voltage to decrease and as a consequence, the TENG will have a lower output voltage. The second reason is the material selection of the TENG, if a TENG has low dielectric strength, it decreases its output. Thirdly, the mechanical stress or deformation of the dielectric due to excessive stretching or straining. The stress or deformation in a dielectric can decrease its electrical properties. This can be caused by excessive pressure between the upper electrode and the dielectric. This can contribute to a decrease in the thickness of the dielectric after a certain number of cycles. The last reason for electrical malfunctions to happen is when the TENG generates excessively high voltages. This can be a result of a large contact area or a high frequency of motion. Hence, both mechanical and electrical properties are essential for the performance of the TENG. All of the reasons need to be taken into consideration when deciding in which environment the TENG is installed. Moreover, the formula states that by increasing the thickness or dielectric strength, it can increase the voltage. Increasing the dielectric strength of a material can be done by altering its composition. However, the scope of the project concentrates on the thickness due to time limitations. For the TENG to function it needs to be able to stop the electrical breakdowns without interrupting the triboelectrification effect. If the intermediate layer is too thick, triboelectrification will be halted; nevertheless, if the intermediate layer is too thin, electrical breakdowns will continue. The thickness-output performance relationship is schematically depicted in Figure 3.

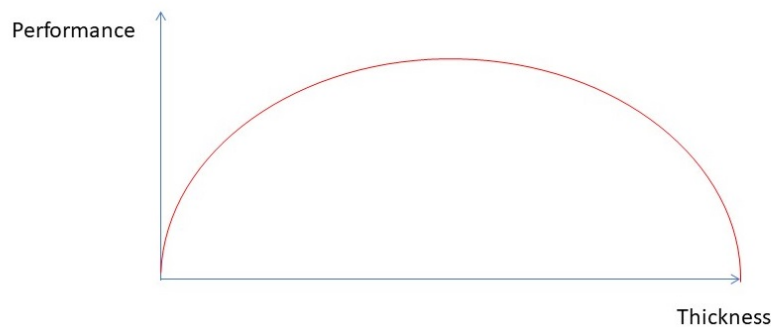


Figure 3: Output performance and thickness relation

4 Problem analysis

4.1 Problem context

For TENGs to be applied on a wide scale of sensors, the output voltage needs to be increased. Currently, a TENG's performance is too low to support a sensor and is therefore used in combination with another type of energy-transferring mechanism [Zhang et al., 2023]. To enhance the efficiency of a TENG, the individual layers need to be very thin [Wu et al., 2021]. However, decreasing the thickness of the electrode decreases its dielectric strength and its charge capacity, which leads to an increase in regional electrical breakdowns, which in turn leads to a decline in output voltage. Regional electrical breakdowns occur when the dielectric polydimethylsiloxane (PDMS) comes in contact with an electrode under a certain voltage, which happens continuously in the system. A solution to decrease the electrical breakdowns is to increase the TENG's dielectric. However, this causes the TENG to be less efficient. The TENG's performance is affected by its flexibility when external mechanical energy is applied to it. One strategy to enhance TENG performance is to add a layer between the electrode and PDMS, the intermediate layer, that inhibits electrical breakdowns.

4.2 Holistic system

The holistic system approach was used to obtain a better understanding of the social and technical influences on this integration project. Engineering and Technology Institute Groningen (ENTEG) consists of several groups, of which the Advanced Production Engineering group (APE) deals with development, implementation and optimization in medicinal and materials engineering. The APE assists with the project by supplying equipment and providing oversight. The TENG will be created and tested using the equipment of APE. If the TENG reaches a certain output voltage, it can be manufactured for two main purposes: energy harvesting and sensors. For energy harvesting, the TENG can be placed, among others, at sound barriers, underwater or in turbulent locations. The other purpose is for the TENG to function as a power supplier for small electronic devices such as sensors. TENG sensors can be used with human interaction, such as by inserting them in shoes, integrating them into clothing, or even directly attaching them to human bodies. The purpose of human-interacted sensors is to collect data for health purposes. Sensors are required in smart objects for them to detect and interpret themselves and the environment. Both sensors gather data for the Internet of Things system. The whole comprehensive system is depicted in Figure 4

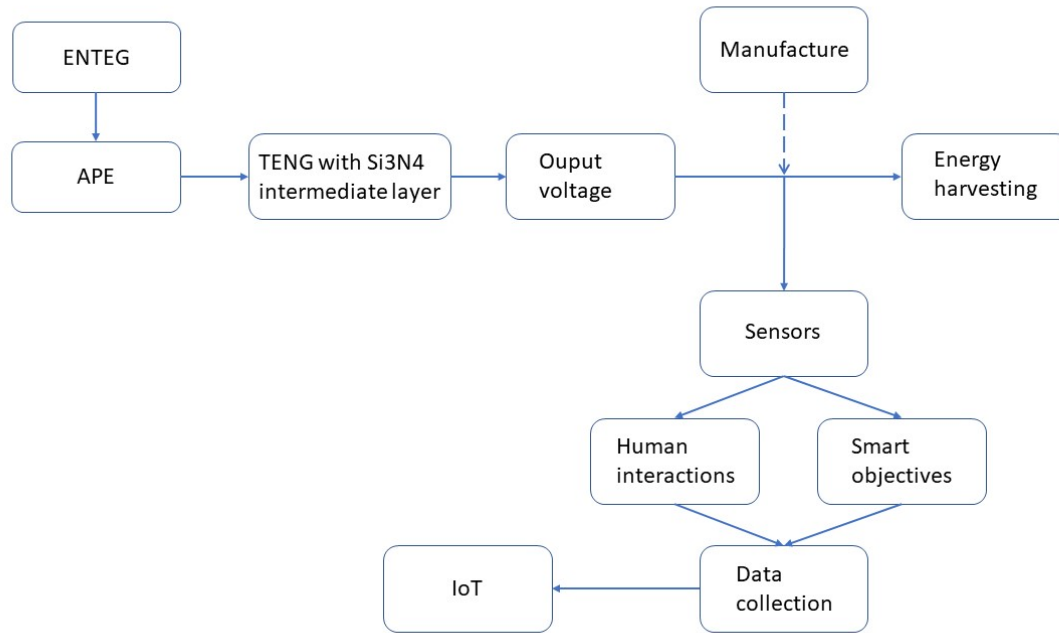


Figure 4: Holistic system approach

4.3 Research objective

The SMART objective of this project is:

To find the ideal thickness of the Si₃N₄ intermediate layer that enhances the TENGs performance, by evaluating previously done research and estimating the possible thicknesses that can enhance the outcomes within ten weeks.

4.4 Research questions

What Si₃N₄ coating thickness enhances the performance of the triboelectric nanogenerator (TENG) compared to previous research?

Q1: What is the effect of different thicknesses of the Si₃N₄ intermediate layer on TENG performance?

Q1.1 How can layers of varying thicknesses of Si₃N₄ be created?

Q2: How are the different properties of the other compounds affecting the performance of a TENG?

Q2.1: How does the thickness of the dielectric layer impact the performance of a TENG?

Q2.2: How does the electrode material affect the performance of a TENG?

5 Intermediate layer

5.1 Design

The design for the TENG used in this research project is a contact separation mode. This project aims to discover the ideal thickness of the intermediate layer and this mode is low in complexity compared to the other modes. The CS-TENG has various designs with either one or two dielectrics. For this research, the choice was made to create a CS-TENG with one dielectric to decrease the complexity further without interfering with the results of the project. To isolate the effects of the Si_3N_4 , all the electrodes as well as the PDMS are set to a constant. This is done by creating all the electrodes at once in the PVD machine and coating the PDMS layer for each thickness at the same time. Taking all the factors into consideration results in the following design, depicted in Figure 5.

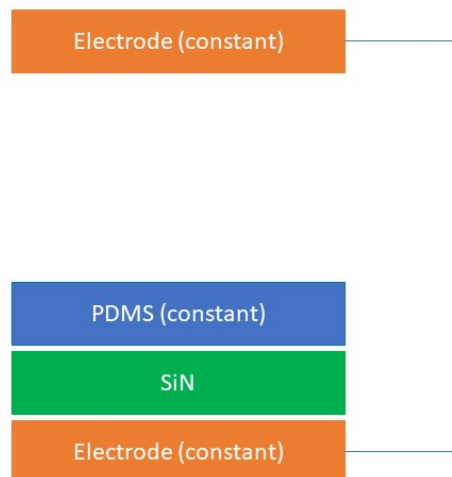


Figure 5: Design of the CS-TENG with Si_3N_4

5.2 The effects of an intermediate layer

To assure performance enhancement, the intermediate layer must be balanced between electron blocking, storing capacity and functioning as an electron transfer layer. To function as an electron-blocking layer, the material has to have high resistivity to increase breakdown voltage. The storage capacity is measured using the charge density of the material. To operate as an electron transfer layer, the material must have a higher work function compared to the electrode. The design of an $MXene/TiO_2$ intermediate layer is depicted in Figure 6 and represents the distinctions between a TENG with and without an intermediate layer.

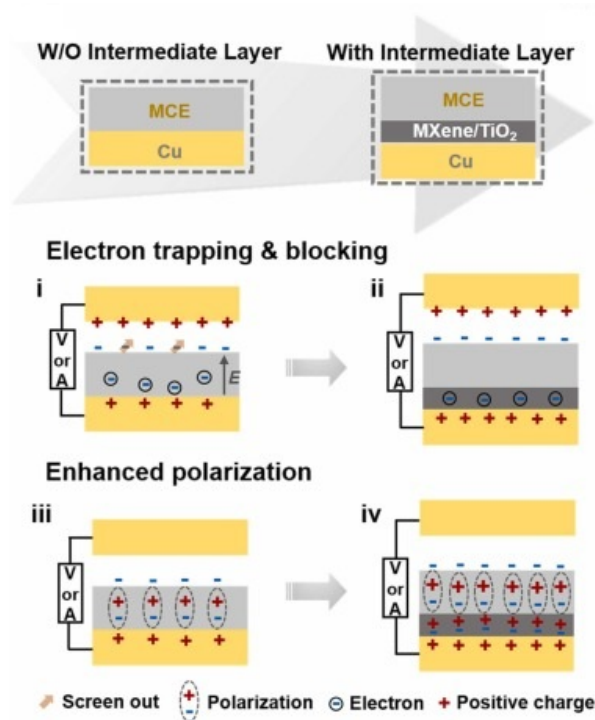


Figure 6: $MXene/TiO_2$ intermediate layer by [Chen et al., 2022]

As seen in 6, the intermediate layer functions as an electron trapping and blocking layer to reduce the electrical malfunctions, which are marked as screened-out electrons. In addition, the figure depicts the enhanced polarisation when using an intermediate layer, which is caused by the increasing permittivity of the material. Furthermore, due to the increasing dielectric strength of an intermediate layer, its breakdown voltage can increase. Hence, the intermediate layer enhances the polarisation and output voltage of the TENG [Xie et al., 2021].

The second parameter to be considered is thickness. For each material, there is one ideal thickness where the intermediate layer is balanced between blocking and transferring electrons. Making the intermediate layer too thick results in a decrease in the induction effect. Making the intermediate layer too thin results in a decrease in blocking electrons, resulting in increased electrical breakdowns.

5.3 Characteristics of materials

5.3.1 Silicon nitride

Si_3N_4 has very high resistivity and is already extensively used in capacitors to enhance charge density [Pierson, 1999]. A TENG with Si_3N_4 as an intermediate layer was already investigated by X. Tao et al., who concluded that the output voltage substantially increased [Tao et al., 2022]. In the experiment, a wearable TENG was created and tested with several intermediate layers; Si_3N_4 produced the maximum output voltage. However, this experiment did not choose to use Si_3N_4 due to its stiffness. This is why Si_3N_4 is not applicable in every situation; it can be used in locations where toughness and high wear resistance are primary factors. Another intermediate layer that was researched and has similar characteristics is SiO_2 , which can function as a conductive charge pathway and has a high charge capacity. In the article by Kim et al., a SiO_2 and Ni coating was tested and resulted in a high-performance enhancement.

5.3.2 Polydimethylsiloxane

PDMS is widely used for micro and nano devices for its high flexibility and chemical stability [Xu et al., 2021] [Sereni, 2016]. It can become polarised and store electricity. PDMS is one of the most investigated materials in the triboelectric series due to its high potential. There have been several experiments done with PDMS as a dielectric layer. For instance, it has been found that soft PDMS generates a higher triboelectric charge owing to the increasing contact surface area [Pandey et al., 2018]. PDMS is applicable for both mechanical energy harvesting and human censoring due to its flexibility and can thus be employed as the dielectric material in the CS-TENG for this project. PDMS is used for this project while other methodologies can enhance the performance. For example, enhancing the flexibility of the PDMS layer by synthesising it with $CaCu_3Ti_4O_{12}@BaTiO_3$ showed an enhanced performance of 480% on V_{oc} , I_{sc} , and Q_{sc} compared to pure PDMS [Lu et al., 2023].

5.3.3 Copper and titanium

Copper (Cu) is commonly used as an electrode in any form of TENG because of its high conductivity and low cost. Because Cu is ranked comparatively low on the triboelectric series, it can readily donate electrons to higher materials, such as PDMS. These characteristics make Cu a feasible electrode to use in this project.

However, the different Cu coatings scattered while adding the Si_3N_4 coating. This resulted in the exploration of titanium (Ti) as a material for the electrode because of its higher adhesion force [Russell et al., 1995]. Moreover, it has similar properties compared to Cu to function as an electrode and is thus a more reliable electrode. However, Ti is a more expensive material due to its rarity and difficulty in manufacturing.

6 Equipment

Various types of equipment can be used to create and test a CS-TENG. The following set of equipment is used to create the CS-TENG for this project which can also be found in Appendix A.

6.1 Physical Vapour Deposition

One of the instruments used in this project is a physical vapour deposition (PVD) machine, which operates in four stages. The first stage is the evaporation of the selected material using an electron beam. The second phase is to transport this vapour to the substrate. Thirdly, there is a reaction between the metal and gas, in this case, argon. The last stage is the deposition of the coating on the substrate surface [Makhlouf, 2011]. For this project, the metals Cu and Si_3N_4 will be deposited on a glass plate. The PVD machine used in this project is the Teer Coatings Limited UDP35014. Different types of parameters can be set in the PVD machine such as bias voltage, target current and gas flow. These parameters influence the fracture composition of the material that gets deposited onto the substrate. The impact of the distance, the bias voltage and the bias frequency in the PVD machine have been researched by Pei et al., which was the foundation for the investigation by Smits to come up with the optimal parameters for this project.

6.2 Spin-coating

The spin-coating machine retains a glass plate via vacuum and when a substance is applied, it rotates to ensure an even distribution. The maximum rotations per minute (RPM) is 3000, but the RPM used for this project is 2000. For this project, two methods were used to produce the PDMS coating. The first one is applying the PDMS substance to the rotating substrate. The other method was to first apply the PDMS to the substrate and initiate the rotation.

6.3 Electrometer

An electrometer is used to measure the three variables (V_{oc} , I_{sc} and Q_{sc}) to analyse the performance of the TENG. The CS-TENG has two copper conductors affixed to the electrodes to which the electrometer will be connected. The measurements will be visualised using the Python script provided by Wenjian. In his script, there is an option to select the results of each variable on various scales.

6.4 Tensile tester

The last piece of equipment used for assessing the CS-TENG is the tensile tester. The tension machine is a hydraulic wedge grip machine that can place tension on the substrates and discharges them, serving as the external mechanical force. The tensile tester can be set to a certain frequency and force. The frequency and force were beforehand verified by Veenstra and set to 1 Hz and 20 N, respectively.

7 Results and discussion

7.1 Coatings

7.1.1 Electrodes and Si_3N_4

Each round of electrode coating started with cleansing the glass plates onto which the layers were deposited. This was done to ensure the materials adhered to the glass substrate and to prevent impurities in the coating. The cleansing process is done by first placing the glass plates in acetone and then in an ultrasonic cleaner for 15 minutes. Afterwards, this procedure was repeated with ethanol instead of acetone in the container. The last stage is to dry-blow each glass substrate. When the glass is ready to be coated, it can be placed on the substrate holders using double-sided heat-resistant adhesive. These holders are then fastened onto a circular-shaped frame that fits in the machine. Before placing the glass in the machine, a few items must be covered with aluminium (Al), such as the frame and other targets inside the PVD machine. The Al prevents the machine from vaporising the other metals inside the machine and stops the frame from getting coated in the vaporising metal. Once all the elements are covered, the glass is set to go into the PVD machine. The PVD machine must vacuum itself before use, which is usually done overnight. The electrode parameters can be filled in on the computer connected to the PVD equipment the next day. A large amount of electrodes can be manufactured in the first batch, since the electrode coatings are the first layer on the upper and lower components. The parameters that are used for both the electrode and Si_3N_4 have been researched by Smits and can be seen in Figure 7.

The next step after the electrode coatings are produced is to place a Si_3N_4 coating on top of the electrode-coated substrate. The first few stages are the same as the electrode-coating. There are a few modifications in the procedure compared to the electrode-coating process. One of them is that nitrogen (N_2) gas is introduced to the PVD machine and the coating will be pulsed onto the substrate instead of continuously vaporising. Also, the number of substrates produced declined to around four. This is because the thickness will be variable for each batch. The ideal thickness of Veenstra was measured to have a 120-min deposition time. The next substrate had 60 and 180-min deposition times, which indicates that the optimal thickness has a deposition time between 60 and 180-min. To narrow down the optimal thickness, are substrates made with a deposition time of 90, 120 and 180-min. The 120-min substrate will be used as a validation point to ensure that the TENG is functioning correctly. Moreover, for the TENG to function, both electrodes need to be connected through a copper wire. Attaching the wire cannot be done when the whole substrate has a Si_3N_4 coating on top of the electrode. This is why the substrate requires partial coverage with Al to partially halt the Si_3N_4 coating.

There were two varieties of coatings used in this project: copper (Cu) and titanium (Ti). The first substrates were produced using Cu, which resulted in some unusable electrodes. The main issue was caused by scattered coating, which can be a result of lower adhesion compared to Ti. Utilizing Ti as an electrode reduced scattering and therefore enhanced the overall performance and reliability of the TENG.

The first stage was to create the Cu coatings of which the results were mixed, not wholly successful. A few were ineffective since the machine ceased rotating during the coating phase. This resulted in a Cu thickness difference between the substrates. Furthermore, the results were altered by the lower adhesive force of Cu compared to Ti. This could be seen in the thickness deviations, where the dense Cu coatings were less likely to adhere to the glass substrate. However, because the majority of the substrates had a coating that could be used in the experiments, Si_3N_4 was applied to those Cu coatings.

Parameters	Cu	SiN
Bias Voltage	40V	60V
Bias Voltage pulse frequency	250 kHz	250 kHz
Bias Voltage pulse width	1500 nsec	1500 nsec
Target unit current	1.5 A	0.8 A
Target pulse frequency	-	250 kHz
Target pulse width	-	1500 nsec
Argon gas flow	15 sccm	15 sccm
Ni gas flow	-	15 sccm
Rotational speed	3.0	3.0
Time	30 min	90/150 min

Figure 7: PVD parameters for the electrodes and Si_3N_4

The results of the first four with a 90-min deposition time Si_3N_4 layer can be seen in Figure 8. The results indicate that the previously mentioned problem with the PVD machine and Cu resulted in a scattering of the upper two substrates. The remaining batches of 120 and 150-min deposition time had the same varied results. The aggregate purity of Cu was too low for most of the substrates. During the testing phase, almost all of the substrates lacked adhesion and portions of the coatings were entirely scattered off the glass substrate. That is why the Cu electrode TENGs will be excluded from the results.

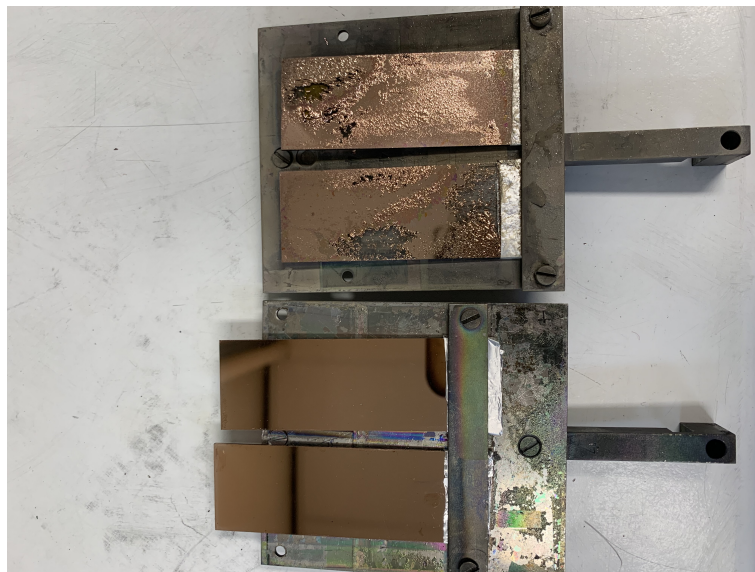


Figure 8: The first samples of Cu with 90-min Si_3N_4 coating

The Ti substrates were of increased quality due to a higher adhesion characteristic compared to Cu. Also, the machine was monitored attentively and did not cease rotating a single time. This resulted in a smoother surface with little to no scattering in the Si_3N_4 coating process, as depicted in Figure 9.

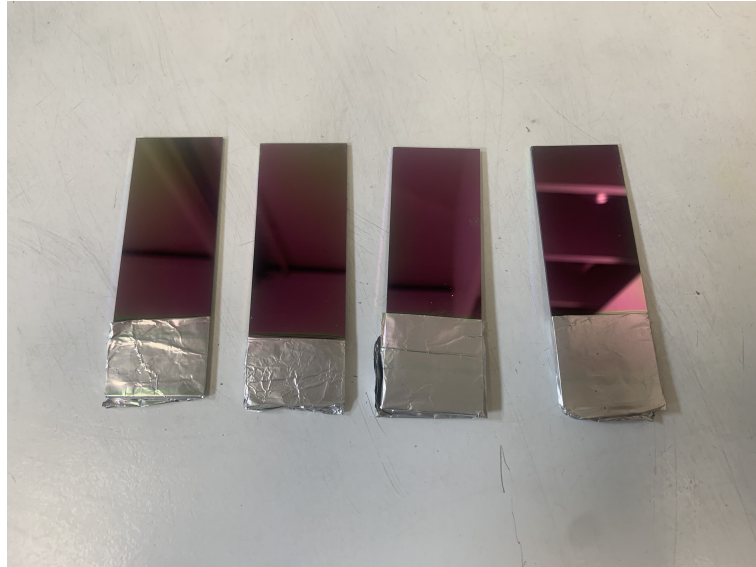


Figure 9: Ti with 90-min Si_3N_4 deposition time

7.1.2 PDMS

The PDMS coating can be made after the Si_3N_4 coatings are made on top of the Cu coating. The procedure consists of a few distinct stages. The first one is combining the silicone elastomer and a curing agent on a 10:1 scale. After agitating this substance for 30 minutes it can be applied to the substrate in the spin-coating machine. This machine is rotating at 2000 RPM and the droplets of PDMS can be applied through an opening in the lid of the machine. 30 droplets of PDMS will be applied to assure equality between the PDMS layers. The next stage is to cure the PDMS coating layer. This is done by situating the substrates for one hour on a plate that is around 100 degrees. The curing period is around two days at room temperature and 45 min at 100 degrees Celsius [Al-Harbi et al., 2018]. The additional 15 minutes are to assure a fully cured PDMS coating.

The substrates with Cu were the first six PDMS coatings created by combining 5 grams of solvent with 2.2 grams of PDMS. The coating was too thin and resulted in an inoperative PDMS coating. The next batch added 1 gram of solvent to 2.75 grams of PDMS, which resulted in operative PDMS coatings.

The first batch of Ti-based substrates was coated with a 2:1 PDMS and solvent ratio, respectively, which resulted in operative TENGs. However, there were a significant number of defects in the coating including several dust particles and some thickness deviations in the PDMS coating. The thickness deviated between 15 and 20 μ m which is a high quantity of deviation that affects performance.

Two modifications helped mitigate the dust and thickness deviation problems of the PDMS coating. First, cover the substrates with aluminium during the curing procedure. During the hardening process, the substrates are placed on a heated plate with the PDMS openly facing upward. The process takes up to an hour and during this time, small portions of dust can fall on the PDMS coating, which leads to a localised decrease in output. The casing helped lower the number of dust particles that get on the PDMS. Secondly, the PDMS was applied to the substrate before spinning rather than while it was spinning. This resulted in a finer surface coating. However, the more evenly distributed PDMS layer also resulted in a decreased thickness of 11 μ m.

7.2 Output results

To isolate the performance of the Si_3N_4 , it is necessary to maintain a constant contact area. This is accomplished by crossing the substrates over each other, resulting in a 6.25cm^2 contact area. This also allows the substrates to be placed on top of each other where the defects are the least.

7.2.1 Results with $11\mu\text{m}$ PDMS coating

The V_{oc} results of the Si_3N_4 with 90-min deposition time indicate the greatest output voltage. The total voltage of the substrate is around 65V which is higher than the results of 120-min with a $12\mu\text{m}$ PDMS layer. The voltage increases by approximately 38% which indicates improved performance when the Si_3N_4 layer has a 90-min deposition time instead of 120-min. Moreover, the voltage of the 120-min deposition time indicates the lowest output, which is a result of more defects compared to the other substrates. Hence, the output should be higher for the 120-min substrate, but it is anticipated not to exceed the 90-min substrate.

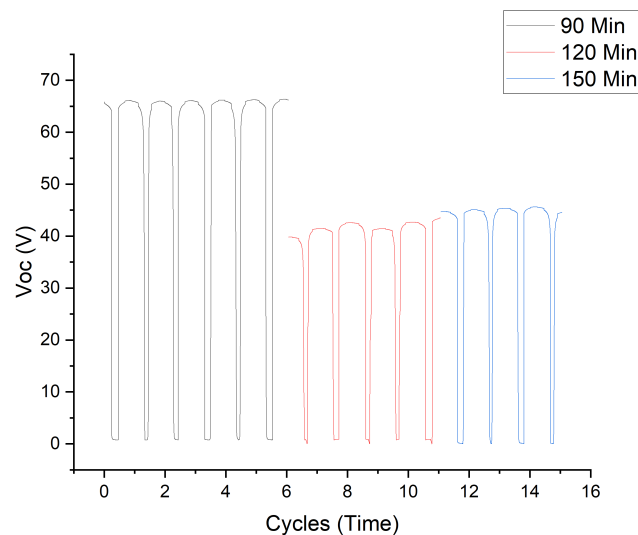


Figure 10: V_{oc} with $11\mu\text{m}$ PDMS coating

The I_{sc} results of the $11\mu\text{m}$ PDMS coating batch showed the greatest output with a 90-min deposition time Si_3N_4 . The output increased by approximately 35% compared to the 120-min substrate. The total ampere generated is very minimal due to the thickness of the PDMS. However, the amount of ampere generated is in the correct area compared to the previously done experiments, whereas the 12 and $10\mu\text{m}$ generate around 8 and $1\mu\text{A}$ respectively. Moreover, the 120-min substrate generates about the same amount of current. This can again be a result of the previously mentioned defects.

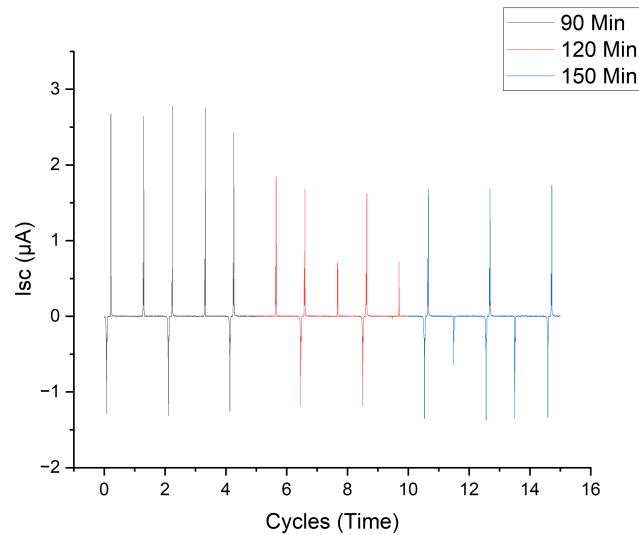


Figure 11: I_{sc} with $11\mu\text{m}$ PDMS coating

The results of the Q_{sc} show that the maximum output originates from the 90-min substrate. The results increased by 20% compared to the 120-min substrate. The 120-min substrate should be around 20nC, according to the results of Veenstra.

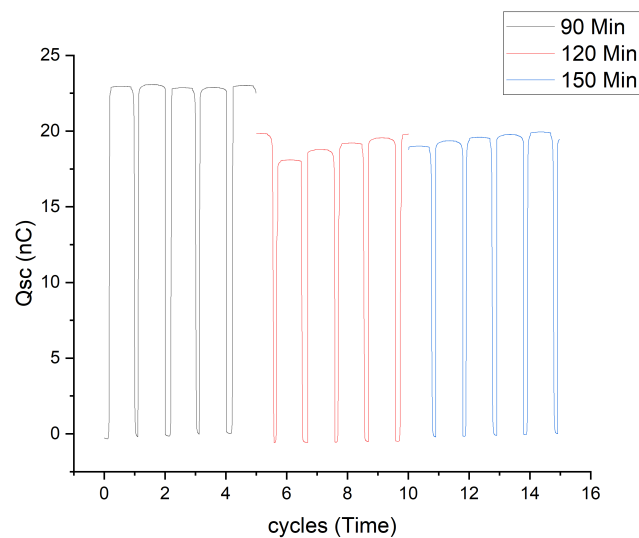


Figure 12: Q_{sc} with $11\mu\text{m}$ PDMS coating

7.2.2 Results with 15~20 μm PDMS coating

The results of the batch with 15~20 μm PDMS coating only consist of two samples since the 120-min substrate had too many defects to work correctly. The defects were too severe in terms of the number of particulates and thickness differences in the PDMS layer. The results of the 120-min substrate were considered to be too low and unreliable. The other two substrates, 90 and 150-min, were closer to the feasible output. The outcomes are much closer to each other compared to the narrower substrates. This can be a result of high thickness deviations within each substrate as well as the quantity of dust and other particles that got trapped on the PDMS coating. Moreover, the V_{oc} results of the 90-min substrate are again the highest.

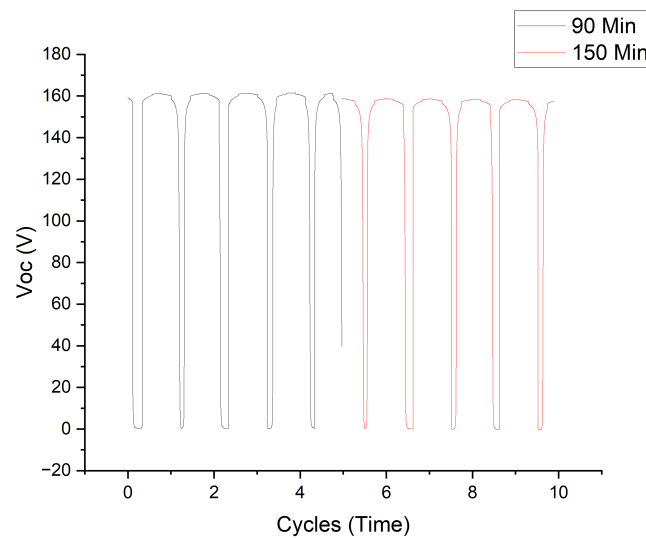


Figure 13: V_{oc} with 15~20 μm PDMS coating

A noteworthy aspect shown in Figure 14 is the difference in the I_{sc} compared to the first substrates. The I_{sc} results show constant output in between the maximum peaks, whereas in section 7.2.1 the current is set to zero. This could be a result of the thickness deviation in the PDMS coating. With a uniform dielectric coating, the current will have a peak right after the separation of the TENG and go to zero because the TENG achieves electrostatic equilibrium again. However, the thickness deviation causes the top electrode to contact the PDMS layer in various regions at different times, the deviation of the PDMS layer itself receives different electrical properties and is therefore causing regional charge differences. The regional charge differences can withhold the TENG from getting into the electrostatic balance. Hence, the additional summits between the greatest peaks.

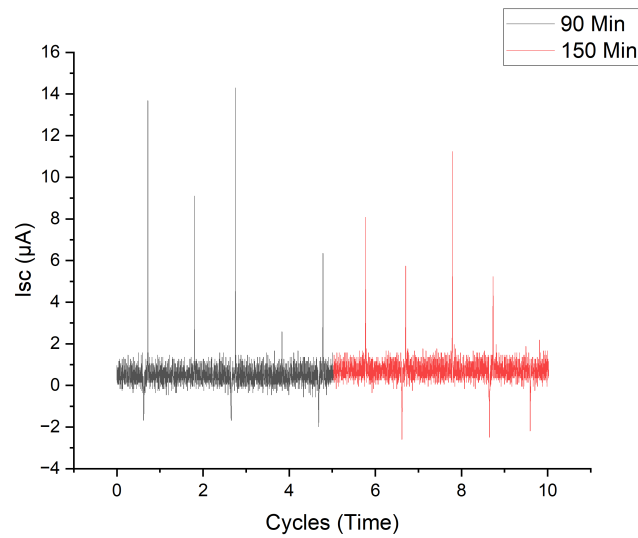


Figure 14: I_{sc} with 15~20 μm PDMS coating

The difference in charge output is not as high compared to section 7.2.1, where the output was around 22 nC, for the 90-min substrate. As shown in Figure 15, the results are around 27.5 nC for the 90-min substrate. This enhancement is significantly lower compared to the V_{oc} and I_{sc} output. However, between the substrates, there is a small enhancement for the 90-min substrate. Combined with the other results, this shows an enhancement of the overall performance of the 90-min substrate.

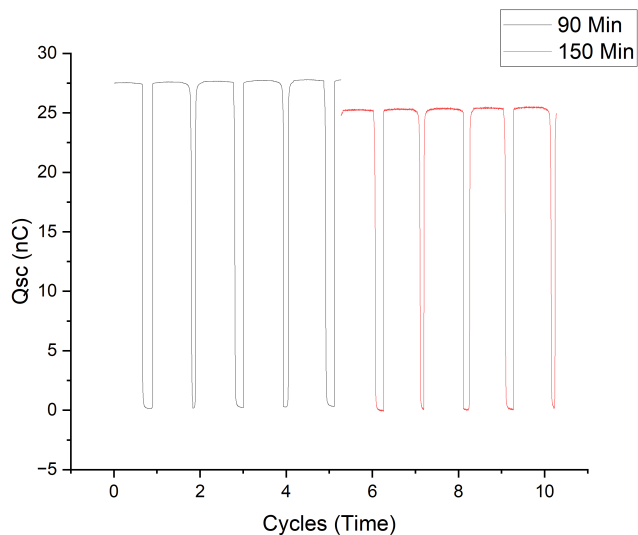


Figure 15: Q_{sc} with 15~20 μm PDMS coating

7.3 Discussion

The results indicate that the 90-min substrate has the highest electron-blocking efficacy. This result is closer to the optimal thickness of the Si_3N_4 intermediate layer compared to the previous results by Veenstra. However, the TENG is still not operating at its maximum potential and can be further enhanced. Moreover, there was only one TENG mode researched, while there are three more TENG modes where the effects of the intermediate layer can result in different performance enhancements. The TENGs developed have a substantial number of defects, which reduce the TENG's performance and, as a result, its validity. For further improvement of the TENG, it should be created in a clean room to exclude defects in the coatings. To assure valid results, all TENGs were examined for thickness and the number of defects. The defects of the TENG consist of the following two factors: dust particles and scattering. Because the PDMS layers vary between 11 and $20\mu\text{m}$ and a typical dust particle is about $5\mu\text{m}$, the composition of the dielectric can be significantly affected. There are several reasons why dust particles decrease the TENG's performance. The attachment of dust particles can result in charge leakage. Dust particles can function as conductive channels; what occurs is that the electrical breakdown voltage is lower compared to the PDMS layer, allowing charge to flow along a low-resistance path. This can reduce charge accumulation on the surfaces, leading to a decrease in the TENG's output voltage and current. Secondly, the surface irregularity of the PDMS layer increases. Dust particles can leave a rough surface on the dielectric material, impacting it in the same way as the variably distributed PDMS coatings, which will be addressed later on in the section. Thirdly, the dust particles may include contaminants that, over time, might chemically react with or deteriorate the dielectric material or other TENG components. This can lead to decreased electrical insulation and changes in material characteristics, among other things, which result in a decline in the overall performance of the TENG. Preventing the attachment of dust particles to the PDMS layer was not possible since the coatings are produced in a non-sterile environment. To minimise the number of dust particles getting affixed to the PDMS layer, it was covered up as much as possible during the curing time and afterwards in plastic containers.

Moreover, the humidity variations during the testing phase in May could vary from 50 to 80% in one day. Humidity can affect the TENG in various ways, such as by interfering with the dielectric strength of a material [Albuquerque and Shea, 2020]. Where excessive humidity, around 90%, resulted in a lower dielectric strength compared to the 10% humidity. When the dielectric strength diminishes, so does the TENG's performance. If humidity fluctuates significantly, so does the performance of the TENG, resulting in an inconsistent output. A long-term influence of humidity can be the degradation of materials. The thin plates of a TENG can corrode rapidly due to the high surface-to-volume ratio of the coatings. This impacts the material composition of the TENG and thus its performance. Excluding the humidity from the TENG could thus enhance the overall performance of the TENG. The group of Vivekananthan et al. enclosed a CS-TENG in a PET casing, resulting in a complete exclusion from humidity. These results demonstrated no declining performance compared to a conventional CS-TENG. This design can enhance the TENG's overall performance further and can also be a promising design for underwater energy harvesting TENGs.

All the TENGs with various Si_3N_4 thicknesses were tested on the same day to minimise the humidity influence between the TENGs. However, all the substrates need up to one hour to test, resulting in a 6- to 7-hour time difference between the first and the last substrate. Between the first and last substrates, the humidity can change substantially. The experiments were executed without a humidity metre in the tested chamber and thus the exact effects of humidity on the substrates cannot be taken

into account. A humidity metre is recommended for future investigations on this issue to thoroughly evaluate the data with humidity effects incorporated. A humid-regulated environment is a preferable alternative for evaluating the substrates, if one is available. Creating a PET casing for the CS-TENG to eliminate the humidity effect is a complicated alternative that will yield different results compared to a humid regulated room. The PET casing TENG is still dependent on the room and its humidity. Therefore, is the humid-regulated room recommended for future research to omit the effect of the humidity in future research.

For the dielectric, the dielectric strength and permittivity are of importance. The dielectric strength will help to prevent electrical breakdowns and the permittivity will help to increase the polarization. Another factor that demonstrated the enhanced performance of the dielectric is its flexibility. The enhanced flexibility achieved by adding $CaCu_3Ti_4O_{12}@BaTiO_3$ to the PDMS layer exhibited an increasing performance of 480% compared to pure PDMS [Lu et al., 2023]. This is a very promising enhancement and could, in combination with an intermediate layer, even further increase the performance of the TENG. While the electrode layers appear to be homogeneous, their surface might have thickness variations on a microscopic level. Improving the flexibility of the dielectric will result in increased contact area at lower thicknesses on a microscopic level. The increased contact area causes a rise in electron transfers, resulting in a higher potential difference.

For the electrode, the properties of the various materials were evident during the Si_3N_4 coating. The scattering of the first batch with Cu had a significant influence on the outcome of the TENG as well as the durability of the electrodes and TENGs. During the Si_3N_4 coating procedure, some of the Cu electrodes were substantially scattered on the edges of the substrate. Ti was used instead of Cu because it has an increased adhesion characteristic, resulting in a collection of electrodes without scattering. This scattering is also due to the environment in which the TENG is created. The coatings were produced on a glass substrate, which has minimal adhesive strength. If the Cu coating is applied to a higher adhesive surface, it will have a higher chance of dispersing. For future research, it is recommended to use an electrode with high adhesive properties to decrease the number of defects during the experiments. The project is based on the fact that triboelectrification is caused by electron transfer, which results in the work function being an essential factor in determining the electrode. Where lower work function results in more electrode transfers, in this case, the work function difference between Cu and Ti is 4.65 eV and 4.33 eV, respectively. This means that using Ti results in a diminution of defects and an increase in electron transfer. However, the cost of Cu is substantially lower compared to Ti.

This project is based on determining the appropriate thickness of the Si_3N_4 layer, while other intermediate layers also demonstrated enhanced performance of the TENG. Materials such as TiO_2 exhibit increasing performance when constructed with Al electrodes and PDMS dielectric. Using the intermediate layer enhanced the output voltage to over 200V [He et al., 2015]. The TENG developed by Veenstra generated close to 200V, suggesting that the change in deposition time and reducing defects might potentially outperform the performance of the TiO_2 intermediate layer.

This integration project was founded on the electron transfer mechanism. However, future research can base its findings on one of the two other transfer mechanisms. For example, enhancing the ion transfer mechanisms can help decrease the accumulation time of the TENG. The accumulation of the V_{oc} with a 90-min deposition time and an $11\mu\text{m}$ PDMS coating can be seen in Figure 16. A variety of factors can affect accumulation, such as charge density. This was researched by Li et al. who

concluded that increasing the charge density, which increases its maximum yield, results in a longer accumulation time. The accumulation time can be decreased by utilising various methods, such as ion injection of the dielectric. This was one of the methods used by Li et al. to decrease the accumulation time. In addition, the accumulation time can also be decreased by implementing an intermediate layer [Cui et al., 2016]. To enhance accumulation time, an intermediate layer can be used in combination with an ion-injected dielectric.

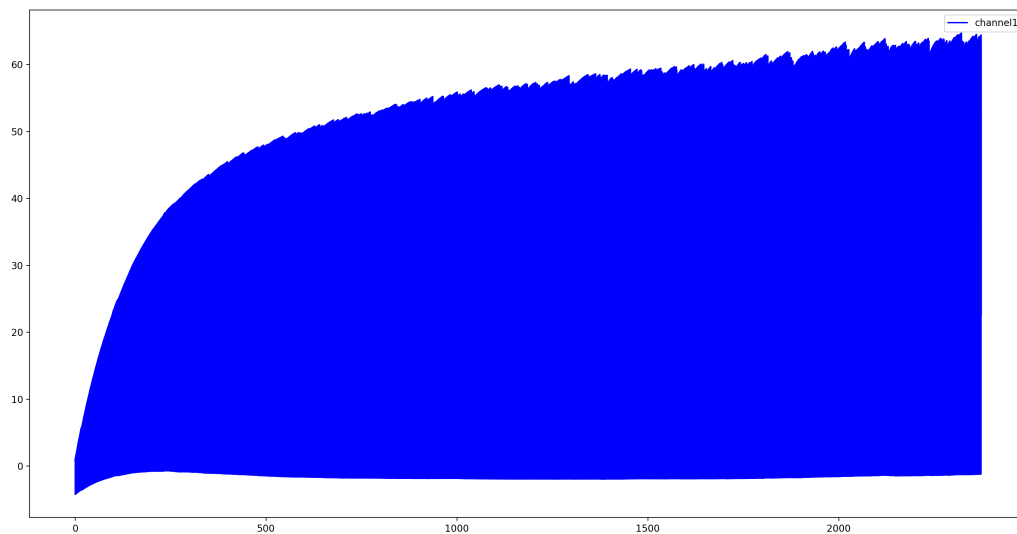


Figure 16: The V_{oc} with a 90-min deposition time and an $11\mu\text{m}$ PDMS coating

Another factor that can affect the performance of a TENG is the composition of the materials, especially the irregularities. The microscopic fractions in the material cause the actual contact surface area to decrease and can induce charge leakage. Figure 17 shows various levels of fractions that are created in a PVD machine by Pei et al. This research was continued by Smits with the results of the optimal bias voltage, distance and all the other parameters for this project. Applying the optimised parameters results in an entirely dense layer that enhances the performance of the TENG. The parameters can be found in Figure 7.

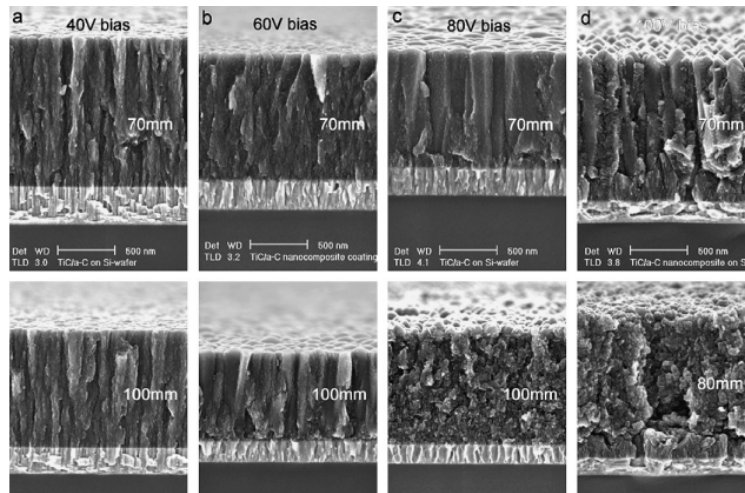


Figure 17: Different bias voltages show distance and for a-d have a bias voltage of 40V, 60V, 80V, and 100V with a two-hour deposition time [Pei et al., 2008]

All the electrodes for the PVD machine were produced using the same parameters, enhancing the equality between the coatings. The same parameters were also used for the Si_3N_4 coating, only the deposition time was different to determine the thickness.

The first sample of PDMS coatings on the Ti substrates resulted in an uneven distribution with a thickness deviation of $15\sim 20\mu m$. The deviations are not the same on every coating, causing the top electrode to encounter a variation of PDMS thicknesses for every substrate and a depletion in the contact area. This resulted in an outcome difference that could get up to approximately 10% between the thinnest and thickest parts. Moreover, this structure deviation causes not only a depletion in performance but also a deviation in I_{sc} compared to the homogeneous PDMS layers. This phenomenon is caused by regional charge differences, which are a result of thickness deviations. The regional charge differences are preventing the TENG from getting into electrostatic balance. This is also causing the Q_{sc} to be lower compared to Veenstra because, when the TENG is in full electrical equilibrium, it can transfer much more charge at once. However, the contact area is substantially decreased by the thickness deviation without a significant loss in V_{oc} or I_{sc} . This can be explained by the hypothesis of Volta-Helmholtz, which states that surface charge can also be enhanced by increasing the contact points. This means that expanding the number of contact points can contribute to increasing the performance of V_{oc} and I_{sc} . While the deviations were not intended for this project, it is feasible that the thickness variations increased the contact points. This resulted in a counterbalance that almost completely compensated for the loss produced by a reduced contact area. This can be fundamental to enhancing the performance of the TENG. An approach is to make the contacted surfaces, the top electrode and dielectric, more porous. This has been done by Vivekananthan et al., who made a porous Ni-foam for the electrode and used sandpaper to enhance the roughness of the dielectric's surface.

This resulted in enhanced performance of V_{oc} and I_{sc} compared to using a flat Al electrode, while the work functions of Ni and Al are 5.01 eV and 4.2 eV, respectively. The performance increased by 37%, while the work function of Ni is higher compared to Al. Moreover, Sriphan and Vittayakorn found that machining rough surfaces between the electrode and dielectric can enhance performance up to three times compared to flat surfaces.

For the overall performance of the substrates, it can be said that the batch with the thickness deviations is an unreliable source to use due to the differences in the substrates. The batch with a more homogeneously distributed PDMS coating is more reliable due to its equality between the substrates. All of the outcome performances are compared to the results of Veenstra to verify their validity. The 11 μm PDMS coating substrates were feasible to conclude the performance enhancement of the 90-min substrates. The thickness of the Si_3N_4 coating is now determined by the deposition duration of the machine. The difficulty of calculating the thickness is caused by the starting and end positions of the substrates, but it can be approximated using Veenstra's thickness. This is based on the fact that the PVD machine sputters on average the same thickness on the substrate every minute, which then results in a 346,5 nm thickness for the 90-min deposition time.

8 Applications of TENG

TENG has a potentially wide application as a micro-nano power source, self-powered sensors, blue energy, and high voltage sources, encompassing areas from medical science to wearable electronics, flexible electronics, security, human-machine interfaces and even environmental science [Wang, 2022]. The TENG created for this project had reliable results that were too low to produce enough electricity for small electronic devices. However, certain adaptations, like increasing the thickness of the PDMS or creating the TENG in a dust-free environment, will result in the ability to charge small electronic devices or provide electricity for sensors. For pressure sensors, usually a power of 10–15 mW is needed [Sachan et al., 2012]. The results of Veenstra show an output voltage around 190 V and a current around 60 μA , which provides 11.4 mW. The power of a device can be calculated by multiplying the voltage by the current. However, the output of the TENG is AC instead of DC and needs to be converted into DC using a rectifier, which can cause a loss of electricity. This is around the minimum required for a pressure sensor, and with the output enhancement discovered in this research, this TENG could probably be used for these types of sensors.

9 Conclusion

The TENG developed during this project had too many defects in the dielectric. However, if produced correctly, it has the potential to outperform other TENGs. The research objective was to discover the ideal thickness, which was unfortunately not found. However, the optimal thickness narrowed down by 50% compared to Veenstra. The performance was measured on three distinct factors: V_{oc} , I_{sc} and Q_{sc} . The results show a performance enhancement on every factor when the TENG has a 90-min Si_3N_4 layer compared to the previously highest performing Si_3N_4 intermediate layer of 120-min. The results are increasingly specific regarding the highest-performing thickness. In this project, the highest-performing thickness is between 60 and 120-min of deposition time. Which is significantly decreased compared to the apex between 60 and 180-min. The performance enhancement is currently measured to be around 20–30% with an $11\mu\text{m}$ PDMS layer. As previously stated, due to unforeseen errors, it was not possible to measure the exact thickness of the intermediate layer. The minutes are not an ideal measurement for future research and it is therefore recommended to determine the exact thickness. This research can be used for future research about the Si_3N_4 intermediate layer to narrow down the optimal thickness even further, as well as to implement the found Si_3N_4 thickness in a variety of TENGs. The overall highest performance of this TENG, with the right PDMS thickness, cannot be calculated and therefore further research needs to be conducted to investigate the precise enhancement. Overall, despite defective dielectrics and lack of precisely determined enhancement, this project highlighted the untapped potential of TENGs and its result can be used in the further development of alternative energy sources.

Bibliography

- Akhtar, F. and Rehmani, M. H. (2015). Energy replenishment using renewable and traditional energy resources for sustainable wireless sensor networks: A review. *Renewable and Sustainable Energy Reviews*, 45:769–784.
- Al-Harbi, L. M., Darwish, M. S., Khowdiary, M. M., and Stibor, I. (2018). Controlled preparation of thermally stable fe-poly (dimethylsiloxane) composite by magnetic induction heating. *Polymers*, 10(5):507.
- Albuquerque, F. B. and Shea, H. (2020). Influence of humidity, temperature and prestretch on the dielectric breakdown strength of silicone elastomer membranes for deas. *Smart Materials and Structures*, 29(10):105024.
- Chen, X., Liu, Y., Sun, Y., Zhao, T., Zhao, C., Khattab, T. A., Lim, E. G., Sun, X., and Wen, Z. (2022). Electron trapping & blocking effect enabled by mxene/tio₂ intermediate layer for charge regulation of triboelectric nanogenerators. *Nano Energy*, 98:107236.
- Cui, N., Gu, L., Lei, Y., Liu, J., Qin, Y., Ma, X., Hao, Y., and Wang, Z. L. (2016). Dynamic behavior of the triboelectric charges and structural optimization of the friction layer for a triboelectric nanogenerator. *ACS nano*, 10(6):6131–6138.
- Deshmukh, K. et al. (2020). 3d and 4d printing of polymer nanocomposite materials.
- He, X., Guo, H., Yue, X., Gao, J., Xi, Y., and Hu, C. (2015). Improving energy conversion efficiency for triboelectric nanogenerator with capacitor structure by maximizing surface charge density. *Nanoscale*, 7(5):1896–1903.
- Kim, J.-K., Han, G. H., Kim, S.-W., Kim, H. J., Purbia, R., Lee, D.-M., Kim, J. K., Hwang, H. J., Song, H.-C., Choi, D., Kim, S.-W., Wang, Z. L., and Baik, J. M. (2023). Electric-field-driven interfacial trapping of drifting triboelectric charges via contact electrification. *Energy Environmental Science*.
- Kim, W.-G., Kim, D.-W., Tcho, I.-W., Kim, J.-K., Kim, M.-S., and Choi, Y.-K. (2021). Triboelectric nanogenerator: Structure, mechanism, and applications. *Acs Nano*, 15(1):258–287.
- Li, Y., Zhao, Z., Liu, L., Zhou, L., Liu, D., Li, S., Chen, S., Dai, Y., Wang, J., and Wang, Z. L. (2021). Improved output performance of triboelectric nanogenerator by fast accumulation process of surface charges. *Advanced Energy Materials*, 11(14):2100050.
- Lu, Y., Qin, Q., Meng, J., Mi, Y., Wang, X., Cao, X., and Wang, N. (2023). Constructing highly flexible dielectric sponge for enhancing triboelectric performance. *Chemical Engineering Journal*, page 143802.
- Makhlouf, A. (2011). Current and advanced coating technologies for industrial applications. In *Nanocoatings and ultra-thin films*, pages 3–23. Elsevier.
- Martins, F., Felgueiras, C., Smitkova, M., and Caetano, N. (2019). Analysis of fossil fuel energy consumption and environmental impacts in european countries. *Energies*, 12(6):964.

- Neusel, C., Jelitto, H., Schmidt, D., Janßen, R., Felten, F., and Schneider, G. A. (2015). Thickness-dependence of the breakdown strength: Analysis of the dielectric and mechanical failure. *Journal of the European Ceramic Society*, 35(1):113–123.
- Pandey, R. K., Kakehashi, H., Nakanishi, H., and Soh, S. (2018). Correlating material transfer and charge transfer in contact electrification. *The Journal of Physical Chemistry C*, 122(28):16154–16160.
- Pei, Y., Chen, C., Shaha, K., De Hosson, J. T. M., Bradley, J., Voronin, S., and Čada, M. (2008). Microstructural control of tic/ac nanocomposite coatings with pulsed magnetron sputtering. *Acta Materialia*, 56(4):696–709.
- Pierson, H. O. (1999). *Handbook of chemical vapor deposition: principles, technology and applications*. William Andrew.
- Rudra, B., Verma, A., Verma, S., and Shrestha, B. (2022). *Futuristic Research Trends and Applications of Internet of Things*. CRC Press.
- Russell, S., Rafalski, S., Spreitzer, R., Li, J., Moinpour, M., Moghadam, F., and Alford, T. (1995). Enhanced adhesion of copper to dielectrics via titanium and chromium additions and sacrificial reactions. *Thin Solid Films*, 262(1-2):154–167.
- Ruys, A. J. (2018). *Alumina ceramics: biomedical and clinical applications*. Woodhead Publishing.
- Sachan, V. K., Imam, S. A., and Beg, M. T. (2012). Energy-efficient communication methods in wireless sensor networks: A critical review. *International Journal of Computer Applications*, 39(17):35–48.
- Sereni, J. G. R. (2016). Reference module in materials science and materials engineering.
- Smits, B. (2023). Optimizing sputtering parameters of pulsed dc reactive magnetron sputtering for depositing Si_3N_4 films for an ultra-durable triboelectric nanogenerator. *Bachelor Integration Project IEM*, 1(1):45–55.
- Song, Y., Wang, N., Wang, Y., Zhang, R., Olin, H., and Yang, Y. (2020). Direct current triboelectric nanogenerators. *Advanced Energy Materials*, 10(45):2002756.
- Sriphan, S. and Vittayakorn, N. (2018). Facile roughness fabrications and their roughness effects on electrical outputs of the triboelectric nanogenerator. *Smart Materials and Structures*, 27(10):105026.
- Tao, X., Zhou, Y., Qi, K., Guo, C., Dai, Y., He, J., and Dai, Z. (2022). Wearable textile triboelectric generator based on nanofiber core-spun yarn coupled with electret effect. *Journal of Colloid and Interface Science*, 608:2339–2346.
- Veenstra, B. (2023). Silicon nitride electron blocking layer for high-performance triboelectric nanogenerators. *Research project Master*, 1(1):45–65.
- Vivekananthan, V., Chandrasekhar, A., Alluri, N. R., Purusothaman, Y., and Kim, S.-J. (2020). A highly reliable, impervious and sustainable triboelectric nanogenerator as a zero-power consuming active pressure sensor. *Nanoscale Advances*, 2(2):746–754.

- Wang, S., Lin, L., and Wang, Z. L. (2012). Nanoscale triboelectric-effect-enabled energy conversion for sustainably powering portable electronics. *Nano letters*, 12(12):6339–6346.
- Wang, Z. L. (2017). On maxwell's displacement current for energy and sensors: the origin of nanogenerators. *Materials Today*, 20(2):74–82.
- Wang, Z. L. (2022). On the expanded maxwell's equations for moving charged media system—general theory, mathematical solutions and applications in teng. *Materials Today*, 52:348–363.
- Wu, C., Wang, A. C., Ding, W., Guo, H., and Wang, Z. L. (2019). Triboelectric nanogenerator: A foundation of the energy for the new era.
- Wu, Z., Chen, J., Boukhvalov, D. W., Luo, Z., Zhu, L., and Shi, Y. (2021). A new triboelectric nanogenerator with excellent electric breakdown self-healing performance. *Nano Energy*, 85.
- Xie, X., Chen, X., Zhao, C., Liu, Y., Sun, X., Zhao, C., and Wen, Z. (2021). Intermediate layer for enhanced triboelectric nanogenerator.
- Xu, Y., Takai, M., and Ishihara, K. (2021). Functional coatings for lab-on-a-chip systems based on phospholipid polymers. In *Handbook of Modern Coating Technologies*, pages 555–595. Elsevier.
- Zhang, Z., Guo, X., Wen, F., Shi, Q., He, T., Dong, B., and Lee, C. (2023). Triboelectric sensors for iot and wearable applications.

Appendices

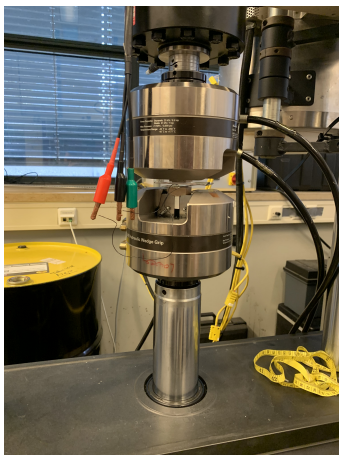
A Equipment used



(a) PVD machine



(b) Spin coating machine



(c) Tensile tester



(d) Electrometer



(e) Stirring and heating plate

Figure 18: Different machines used this project

B Results Bas Veenstra

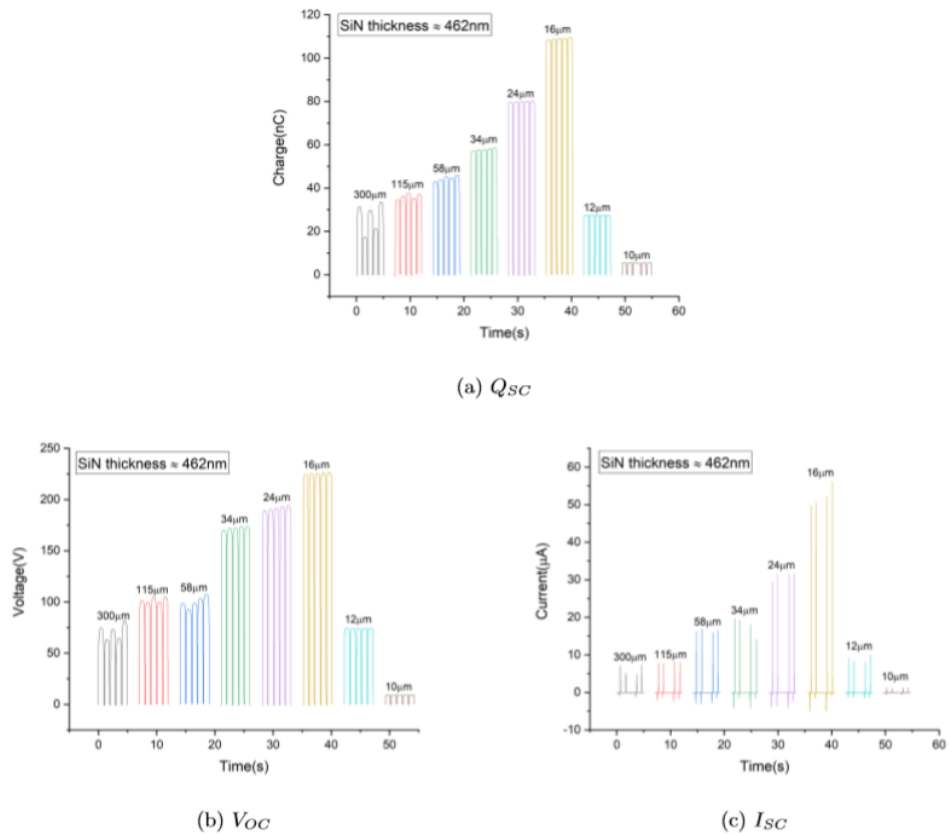


Figure 19: Results of Bas Veenstra with different PDMS thicknesses

Acknowledgement

This integration project would not have been possible without my supervisor Y. (Yutao) Pei, W. (Wen-jian) Li and the APE team. The available equipment and their expert advice were the foundation of this integration project. I am also great full to Dr. A.J. (Albert) Bosch for his encouragement and support on the report. In addition, I would like to thank B. Veenstra, whose methods and results were fundamental to this integration project, as well as his support.